Performance Improvement of Mechanically Beam-Steerable Transmitarray Antennas by Using Offset Unifocal Phase Symmetry

Mei, Peng; Pedersen, Gert Frølund; Zhang, Shuai

Published in:
I E E E Transactions on Antennas and Propagation

Publication date:
2022

Document Version
Accepted author manuscript, peer reviewed version

Performance Improvement of Mechanically Beam-Steerable Transmitarray Antennas by Using Offset Unifocal Phase Symmetry

Peng Mei, Gert Frølund Pedersen, and Shuai Zhang

***Abstract*— This paper presents the concept of offset unifocal phase symmetry to improve the performance (gain, gain roll-off, sidelobe level, etc.) of mechanically beam-steerable transmitarray (TA) antennas. The phase shifts are initially determined from an offset feed source to make the corresponding TA antenna radiate a tilted beam with high gain. The phase shifts are asymmetric and can be broadly divided into dominant and ordinary phase shifts with respect to the offset feed source. By mirroring the dominant phase shifts to make the phase shifts symmetric, it can enable symmetric radiation beams for symmetric offset feed sources and improve phase error. When the offset feed source is moving inward to steer the main beam, the phase error of the phase-shifting surface with respect to the feed source starts to occur, while the electric-field spillover/ illumination from the feed source is improved, which can maintain the gains of scanning beams. To verify the validity of the concept, the performance of a beam-steerable TA antenna enabled by the offset unifocal phase symmetry has been simulated and compared with the counterparts of unifocal and bifocal beam-steerable TA antennas. The measured results agree well with the simulated ones, revealing that the beam-steerable TA antenna enabled by the offset unifocal phase symmetry can maintain realized gains of scanning beams, suppress sidelobe levels, and reduce gain roll-off within the beam-scanning coverage. The offset unifocal phase symmetry, in principle, is a generalized approach and applicable to reflectarray antennas to improve the beam-steerable performance as well.**

***Index Terms*— Transmitarray antenna, gain roll-off, bifocal, sidelobe level, offset unifocal phase symmetry.**

I. Introduction

Beam-steerable antennas capable of flexibly steering radiation beams are good candidates to perform communications with mobile users to maintain link budget and offer reliable connections, especially at the millimeter-wave bands [1], [2]. Due to the simple configuration, high gain, and low loss of transmitarray (TA) and reflectarray (RA) antennas, they have been widely investigated in the past decades, where both TA and RA antennas consist of a phase-shifting surface and a feed source. TA and RA antennas can do beam steering by either electrical or mechanical control solutions. For the electrical control, it is typically implemented by loading RF components (e.g., PIN diode, etc.) on each unit cell to achieve tunable transmission/reflection phases by controlling DC bias [3]-[8]. The electrical control solution, however, suffers from high cost, high loss, and high complexity.

For passive TA and RA antennas, each unit cell only offers a fixed phase shift once its dimensions are determined. Nonetheless, the beams of passive TA and RA antennas can be mechanically steered by moving the feed source [9]-[12], using multiple feed sources [13]-[17], rotating the phase-shifting surface [18], [19], or rotating the unit cells of the phase-shifting surface [20], [21]. Among them, the movement of the feed source (equivalent to multiple feed sources) or rotating the phase-shifting surfaces introduces certain progressive phase gradients with respect to the feed source, thereby tilting the beams of the TA and RA antennas. The significant gain roll-off and remarkable sidelobe level degradations always occur when the feed source is moving outward to steer the beams of the TA and RA antennas whose phase-shifting surfaces are usually built according to the illumination of the center-located feed source (unifocal TA antenna). To improve the gain roll-off, bifocal phase synthesis and phase-optimization-based methods have been proposed and leveraged [10], [22]-[24] to find the desired phase shifts to implement the phase-shifting surfaces. The bifocal phase synthesis can formulate explicit expressions to mathematically calculate the phase shift that each unit cell should offer. It is observed that the bifocal phase synthesis can indeed lower the gain roll-off but at the expense of reduced gains of scanning beams. The phase-optimization-based method, by contrast, can define objective and cost functions, aiming at achieving a minor gain roll-off and comparable gains within the beam-scanning coverage with powerful algorithms [10], [24]. It, however, is time-consuming as extensive iterative computations are needed to achieve the goals.

In this paper, the concept of offset unifocal phase symmetry is proposed and studied to improve the performance (e.g., gain, gain roll-off, sidelobe level, etc.) of mechanically beam-steerable TA antennas. The concept further compromises the phase error and electric-field spillover/illumination to maintain the gains of scanning beams and minimize the gain roll-off within the beam-scanning coverage by mirroring the dominant phase shifts. When the offset feed source is moving towards the center position to steer the beam, the phase error of the phase-shifting surface starts to happen, and the electric-field spillover/illumination of the feed source to the phase-shifting surface is improved. As a result, the improved electric-field spillover/illumination could compensate for the gain loss caused by the phase error, resulting in stable and high-gain scanning beams. For proof of the concept, three beam-steerable TA antennas enabled by unifocal synthesis, bifocal synthesis, and the proposed concept have been simulated, compared, and measured. The measured results agree well with the simulated ones, verifying the effectiveness of the offset unifocal phase symmetry in terms of improving the performance of mechanically beam-steerable TA antennas.

The main contribution of this paper is to propose the concept of offset unifocal phase symmetry. It does not rely on any algorithm but can specify explicit procedures to determine the desired phase shifts to implement the phase-shifting surfaces of mechanically beam-steerable TA/RA antennas. The beam-steerable TA antenna enabled by the offset unifocal phase symmetry can achieve higher gains compared to the bifocal phase synthesis, reduced gain roll-off compared to the unifocal phase synthesis, and highest gains when the main beam is steered to a large angle compared to both. Moreover, the phase symmetry concept can be further extended to make some asymmetric components (e.g., electric field, phase, etc.) symmetric to obtain symmetric performance as explicitly discussed in Section IV.

The remainder of the paper is organized as follows: Section II elaborates on the concept of offset unifocal phase symmetry, and the performance of the three beam-steerable TA antennas is compared in terms of realized gain, gain roll-off, and sidelobe level. The three beam-steerable TA antennas have been measured in Section III. Section IV discusses the generality of the offset unifocal phase symmetry and the extension of the concept of phase symmetry. Some

Manuscript received January 2022. The work is partly supported by MARS2 project (*Corresponding author: Shuai Zhang*)

The authors are all with the Antennas, Propagation and Millimeter-wave Systems (APMS) Section, Department of Electronic Systems, Aalborg University, Aalborg, 9220, Denmark. (Email: mei@es.aau.dk, sz@es.aau.dk, gfp@es.aau.dk)

conclusions are finally drawn in Section V.

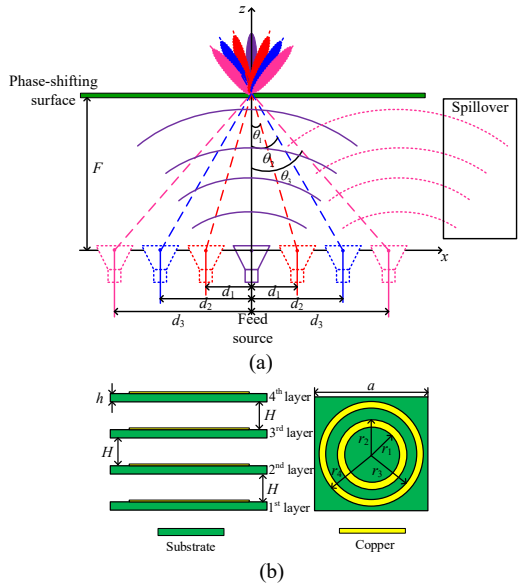

Fig.1. (a). The diagram of the mechanically beam-steerable TA antenna by moving the feed source along a straight line. (b). Unit cell structure used for phase shift. (h = 0.508 mm, H = 2.0 mm, a = 5 mm, r_4 = 2.3 mm, r_3 = 1.8 mm, r_2 – r_1 = 0.5 mm, Rogers RO4350B is adopted as the substrate.)

II. Concept of Offset Unifocal Phase Symmetry and Beam-Steerable Performance Comparison

The beam-steerable TA antennas discussed in this paper mainly rely on the mechanical movement of the feed source along a straight line as illustrated in Fig. 1. The movement of the feed source with respect to a fixed phase-shifting surface can introduce a certain phase gradient, thereby tilting the main beam of the TA antenna. It is also found that the direction of the tilted beam is closely associated with the spatial distance of the feed source and phase-shifting surface (F), and the displacement of the offset feed source (d_i, i = 1, 2, 3 in this paper), which is approximately constrained by the following equation:

$$\theta_i \approx \arctan(\frac{d_i}{F}), \quad i = 1,2,3 \tag{1}$$

Eq. (1) can be viewed as a rule of thumb to specify the scan range that a beam-steerable TA antenna can reach by mechanically moving the feed source along a straight line when the size of the phase-shifting surface is fixed. Also, the tilted angle in bifocal phase synthesis should be less than the angle calculated with Eq. (1) to maintain a good gain roll-off when the spatial positions of the feed source and phase-shifting surface are known as reported in [10] and [14]. The proposed offset unifocal phase symmetry also follows this rule.

Without loss of generality, the four-layered and double-ring structure is chosen as the unit cell to build the phase-shifting surfaces for TA antennas described in this paper as shown in Fig. 1(b). The detailed features and the frequency response of the unit cell can be found in [25], where some dimensions are slightly modified in this work. It should be mentioned here other unit cells capable of both high transmission and phase shifts are also applicable to implement the phase-shifting surfaces for TA antennas.

The feed source used here is a linearly-polarized horn antenna with a model of "PASTERNACK PE9851/2F-10", operating from 22 GHz to 33 GHz with a nominal gain of 10 dBi [26]. According to the radiation patterns of the horn antenna at 25.0 GHz, also taking the aperture efficiency, simulation time, and maximum scanning angle constrained by Eq. (1) into consideration, the vertical distance between the phase center of the feed source and the phase-shifting surface (F) is chosen as 100 mm and the size of the phase-shifting surface is selected as 200 mm × 200 mm, resulting in an F/D of 0.35. In this case, the radiation beam of the mechanically beam-steerable TA antenna will direct to around 10°, 20°, and 30°, when the feed source moves outward 20 mm, 40 mm, and 60 mm, respectively. All simulations in this paper are carried out with CST Microwave Studio Software, where the Time Domain Slover, the mesh type of Hexahedral with an accuracy of -40 dB, the cells per wavelength of 20, and cells per max model box edge of 25 are adopted to maintain sufficient simulation accuracy.

A. Concept of offset unifocal phase symmetry.

For the unifocal beam-steerable TA antenna, when the feed source is moved outward, the gain roll-off within the beam-scanning coverage is attributed to the following two aspects: a). the phase error of the phase-shifting surface with respect to the moving feed source increases; b). the electric-field spillover/illumination on the phase-shifting surface from the offset feed source decreases, where the latter can be observed in Fig. 1(a). Moreover, the effects of the two aspects become more significant when the main beam steers to a large angle (a large displacement of the feed source). Here, the spillover and illumination efficiencies of the feed source with respect to the phase-shifting surface are calculated according to the theoretical analysis reported in [27] when the feed source moves outward with an interval of 20 mm as summarized in Tab. I.

Tab. I. The spillover and illumination efficiencies with different displacements of the feed source at 25.0 GHz

Displacement	0	± 20 mm	± 40 mm	± 60 mm
Beam direction	0°	± 10°	± 20°	± 30°
Spillover efficiency	0.8552 (-0.68 dB)	0.8302 (-0.80 dB)	0.7547 (-1.22 dB)	0.6559 (-1.83 dB)
Illumination efficiency	0.8016 (-0.96 dB)	0.7925 (-1.01 dB)	0.758 (-1.20 dB)	0.7121 (-1.47 dB)
Loss of spillover and illumination	1.64 dB	1.81 dB	2.42 dB	3.30 dB

As seen in Tab. I, both spillover and illumination efficiencies are decreased when the feed source is moving outward. Inspired by the relation between the spillover/illumination and displacement of the feed source, the phase-shifting surface could be configured according to the phase shifts resulting in a high gain and tilted radiation beam for an offset feed source. When the feed source is moving inward, the phase error starts to occur, while the spillover/illumination efficiency will be improved. The improved spillover/illumination efficiency could possibly compensate for the gain loss caused by the phase error, thereby maintaining the gains of scanning beams. The concept of offset unifocal phase symmetry is therefore proposed and explained with a specific case in the following.

Here, the feed source offset by – 60 mm (d_3 = - 60 mm) is selected. First, the phase shifts on the plane of the phase-shifting surface are calculated and shown in Fig. 2(a). These phase shifts will result in a main beam of the corresponding TA antenna at the broadside direction despite the feed source being offset. To tilt the main beam to + 30°, a progressive phase gradient shown in Fig. 2(b) should be added to Fig. 2(a) to obtain the final phase shifts shown in Fig. 2(c).

Then, the radiation beam of a TA antenna whose phase-shifting surface is configured according to the phase shifts in Fig. 2(c) has been simulated and shown in Fig. 3, where the main beam tilted + 30° with a realized gain of 29.8 dBi at 25 GHz can be observed. As the phase shift shown in Fig. 2(c) is not symmetric with respect to x = 0, the

asymmetry will lead to the following issues: a). Increase phase error significantly when the feed source is moving toward the center position; b). The radiation beam is not symmetric when the feed source is at the center position; c). The radiation beams are not symmetric for symmetric offset feed sources.

To demonstrate the first two issues mentioned above, the radiation beams of the beam-steerable TA antenna with the phase-shifting surface implemented according to the phase shifts shown in Fig. 2(c) are simulated and plotted in Fig. 3(a) when the feed sources are offset by – 60 mm and at the center position, respectively. As seen in Fig. 3(a), the main beam at the broadside direction is indeed not symmetric, and the gain roll-off when the main beam is steered from +30° to 0° is around 2.5 dB. It implies that the gain enhancement from the improved spillover/illumination efficiency is not sufficient to compensate for the gain loss caused by the phase error which is significant due to the asymmetric phase shifts.

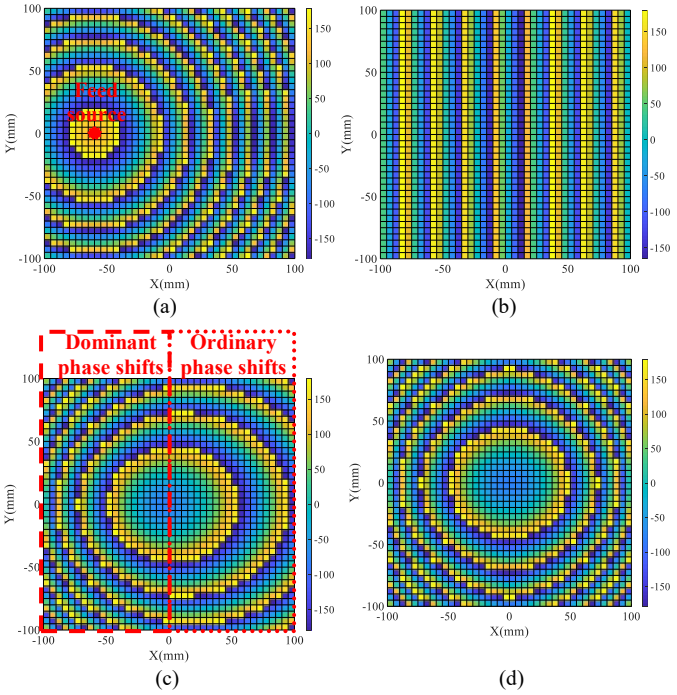

Fig. 2. The evolution of the phase shifts at 25 GHz. (a). The phase distribution when the feed source is located at d_3 = -60 mm. (b). The progressive phase distribution at 25 GHz with a tilted angle of 30°. (c). The phase distribution by adding the phase shown in (a) to (b). (d). The phase distribution by mirroring the dominant phase shifts with respect to x = 0 mm.

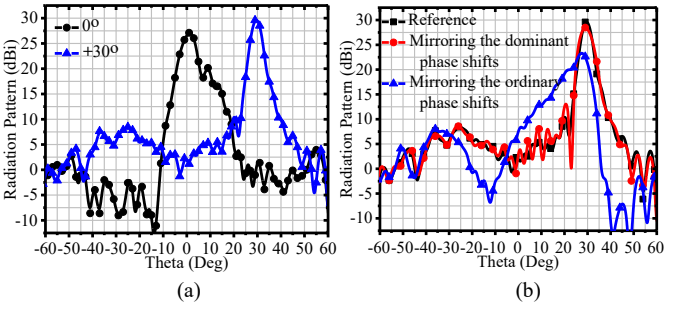

Fig. 3. (a). The radiation beams of the beam-steerable TA antenna with the phase-shifting surface implemented with the phase shifts shown in Fig. 3(c) when the feed source is offset by -60 mm and at the center position. (b). The radiation beams of the beam-steerable TA antennas with the phase shifts shown in Fig. 3(c) as a reference and mirroring the dominant or ordinary phase shifts with respect to x = 0 mm.

As the phase shifts shown in Fig. 2(c) are related to the feed source offset by – 60 mm and are not symmetric with respect to x = 0 mm, the phase shifts in the area of x < 0 mm are therefore called dominant phase shifts as the offset feed source mainly illuminates the unit cells in this area, while the phase shifts located in the area of x > 0 mm are named ordinary phase shifts. The phase symmetry is adopted here to obtain symmetric phase shifts by mirroring the dominant phase shifts with respect to x = 0 mm which can be mathematically formulated with the following expression:

$$\varphi_f(i,j)=\begin{cases}\varphi(i,j), & -100\le i\le -1, and\ -100\le j\le 100\\ \varphi(-i,j), & 1\le i\le 100, and\ -100\le j\le 100\end{cases} \quad (2)$$

As a result, the phase shifts shown in Fig. 2(c) are modified to the one shown in Fig. 2(d) which is now symmetric with respect to x = 0 mm. Here, the effects of mirroring the dominant phase shifts on the radiation patterns (realized gain and sidelobe level) of the corresponding TA antennas with the offset feed source are examined. As seen in Fig. 3(b), mirroring the dominant phase shifts can lead to a gain reduction of around 1.1 dB and a relatively higher sidelobe level that is still below -16 dB. Additionally, the radiation beam of the corresponding TA antenna by mirroring the ordinary phase shifts with respect to x = 0 mm is also checked and plotted in Fig. 3(b) for comparison when the feed source is still offset by – 60 mm. As can be seen in Fig. 3(b), mirroring the ordinary phase shifts with respect to x = 0 mm cannot contribute to performance improvement. The phase shifts shown in Fig. 2(d) can also guarantee a symmetric radiation beam when the feed source is moved to the center position and symmetric tilted radiation beams for symmetric offset feed sources.

B. Comparisons of the beam-steerable performance of the three beam-steerable TA antennas.

In this subsection, the performance of the beam-steerable TA antenna enabled by the offset unifocal phase symmetry is simulated and compared with the counterparts of unifocal and bifocal beam-steerable TA antennas in terms of realized gain, gain roll-off, and sidelobe level, verifying the validity of the offset unifocal phase symmetry in the improvement of beam-steerable performance.

To have a fair and reasonable comparison, the phase-shifting phases of the three beam-steerable TA antennas are implemented with the same type of unit cells shown in Fig. 1(b), and the sizes of the three beam-steerable TA antennas, the distances between the phase-shifting surfaces and the phase center of the feed sources, and feed sources are all the same. The radiation patterns of each beam-steerable TA antenna are simulated and demonstrated when the feed source is offset by ± 20 mm, ± 40 mm, and ± 60 mm. As seen in Fig. 4, all TA antennas can steer the main beams within a beam-scanning coverage of 60° (from -30° to + 30°). Tab. II summaries some metrics of the three beam-steerable TA antennas at 25 GHz, the beam-steerable TA antenna enabled by the offset unifocal phase symmetry can achieve a higher realized gain (an average realized gain of around 29 dBi) compared to that (an average realized gain of 24.8 dBi) of the bifocal beam-steerable TA antenna and also result in a smaller gain roll-off (1.6 dB) compared to that (5.3 dB) of the unifocal beam-steerable TA antenna. The sidelobe levels (the worst value of -15.5 dB) of scanning beams of the beam-steerable TA antenna enabled by the offset unifocal phase symmetry are all better than the counterparts (the worst value of around -8.5 dB) of the unifocal and bifocal beam-steerable TA antennas. The cross-polarization (cross-pol.) levels of the three beam-steerable TA antennas are also checked in all cut planes at 25.0 GHz when the main beam is steered from 0° to 30°, where the worst cross-pol. level is still below -20.0 dB. When the cross-pol levels in the cut plane where the main beam is steered are only considered, they are

quite low (below -100.0 dB) for the three beam-steerable TA antennas when the main beam is steered from 0º to 30º.

Tab. II also presents and compares the loss budgets of the three beam-steerable TA antennas when the main beam is steered from 0º to +30º. The loss budget mainly consists of spillover loss, illumination loss, the loss of phase-shifting surface (including the conduction loss, dielectric loss, and reflection loss.), and the loss of phase error. It should be mentioned here the spillover and illumination losses of the three beam-steerable TA antennas are the same when the feed sources are at the same displacements, which can be found in Tab. I. As seen in Tab. II, the total efficiencies of the three beam-steerable TA antennas are all over 89 % when the main beam steers from 0º to 30º, which can be evaluated from the losses of the phase-shifting surfaces that are all smaller than 0.51 dB. When the main beam is at the broadside direction, the phase error of the unifocal beam-steerable TA antenna is smaller than that of the bifocal and proposed beam-steerable TA antennas. With the main beam steering to a large angle, the relative phase error of the unifocal beam-steerable TA antenna increases significantly, while the bifocal and proposed beam-steerable TA antennas can maintain the phase error. Due to the bifocal phase synthesis fully balancing the phase error and spillover/illumination loss to maintain the minimal gain roll-off, the phase error of the bifocal beam-steerable TA antenna is relatively high. According to the realized gains of the unifocal, bifocal, and proposed beam-steerable TA antennas at 25.0 GHz, the corresponding aperture efficiencies are 40.5 %, 11.0 %, and 28.5 %, respectively.

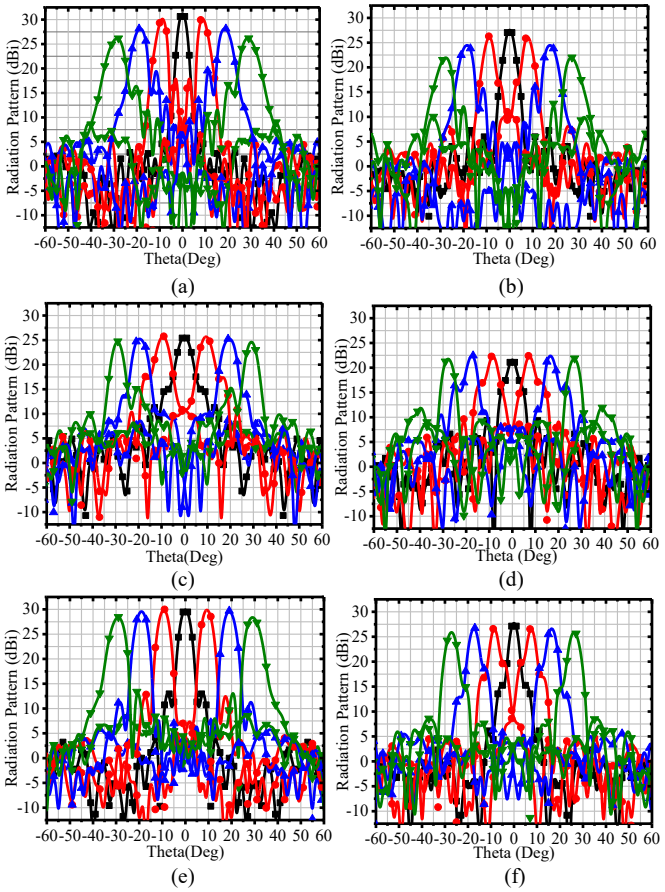

Fig. 4. The simulated radiation beams of the three beam-steerable TA antennas. (a). Unifocal beam-steerable TA antenna at 25.0 GHz. (b). Unifocal beam-steerable TA antenna at 28.0 GHz. (c). Bifocal beam-steerable TA antenna at 25.0 GHz. (d). Bifocal beam-steerable TA antenna at 28.0 GHz. (e). Offset unifocal phase symmetry enabled beam-steerable antenna at 25.0 GHz. (f). Offset unifocal phase symmetry enabled beam-steerable antenna at 28.0 GHz.

Table. II. Performance comparison and loss budget of the three beam-steerable TA antennas at 25.0GHz

	Unifocal beam-steerable TA antenna	**Bifocal beam-steerable TA antenna**	**Proposed beam-steerable TA antenna**
Realized gain	31.5dBi at 0º 30.3dBi at ±10º 28.2dBi at ±20º 26.2dBi at ±30º	25.80 dBi at 0º 25.77dBi at ±10º 25.28dBi at ±20º 24.4dBi at ±30º	**30.0dBi at 0º** **30.0dBi at ±10º** **29.7dBi at ±20º** **28.4dBi at ±30º**
Loss of phase-shifting surface	0.51 dB at 0º 0.37 dB at ±10º 0.36 dB at ±20º 0.34 dB at ±30º	0.34 dB at 0º 0.32 dB at ±10º 0.35 dB at ±20º 0.30 dB at ±30º	**0.34 dB at 0º** **0.32 dB at ±10º** **0.33 dB at ±20º** **0.32 dB at ±30º**
Phase error	1.75dBi at 0º 2.92dB at ±10º 4.42dB at ±20º 5.56dB at ±30º	7.62 dB at 0º 7.50 dB at ±10º 7.35 dB at ±20º 7.40 dB at ±30º	**3.42 dB at 0º** **3.28 dB at ±10º** **2.95 dB at ±20º** **3.38 dB at ±30º**
Gain roll-off	5.3dB (-30º to +30º)	1.4dB (-30º to +30º)	**1.6dB** **(-30º to +30º)**
Sidelobe level	-28dB at 0º -17.5dB at ±10º -8.5dB at ±20º -9.5dB at ±30º	-10.8dB at 0º -8.2dB at ±10º -11.4dB at ±20º -9.3dB at ±30º	**-17dB at 0º** **-17.5dB at ±10º** **-17.5dB at ±20º** **-15.5dB at ±30º**
Cross-pol. level	-23.5dB at 0º -20.4dB at ±10º -20.1dB at ±20º -22.0dB at ±30º	-25.1dB at 0º -21.2dB at ±10º -21.1dB at ±20º -20.3dB at ±30º	**-23.0dB at 0º** **-22.1dB at ±10º** **-21.5dB at ±20º** **-21.2dB at ±30º**

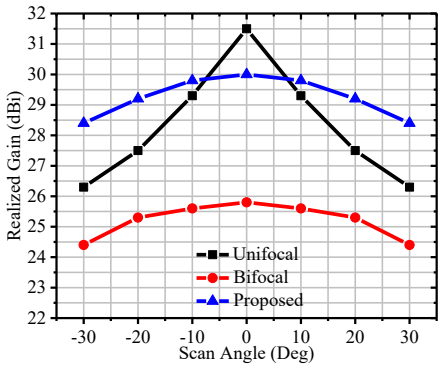

Fig. 5. Simulated realized gains of the three beam-steerable TA antennas with different scan angles at 25 GHz.

To evaluate the effects of the offset unifocal phase symmetry on the bandwidth of the corresponding beam-steerable TA antenna, the radiation patterns of the three beam-steerable TA antennas at 28.0 GHz are also presented in Fig. 4. It is observed that the beam-steerable TA antenna enabled by the offset unifocal phase symmetry can still realize a higher realized gain compared to that of the bifocal beam-steerable TA antenna, and a lower gain roll-off compared to that of the unifocal beam-steerable RA antenna as well. Also, the effects of the offset unifocal phase symmetry on the co-polarization (co-pol.) and cross-pol. levels of the corresponding beam-steerable TA antenna are checked. It is found that the co-pol. and cross-pol. levels can be maintained from 24 GHz to 28 GHz. Moreover, the realized gains of the three beam-steerable TA antennas with different scan angles at 25 GHz are also plotted and compared as shown in Fig. 5, where the proposed beam-steerable TA antenna can offer higher realized gains when the scanning beam steers to a large angle.

III. Experimental Measurement

The three beam-steerable TA antennas described in Section II have

been fabricated and measured to validate the effectiveness of the offset unifocal phase symmetry. The prototypes of the three beam-steerable TA antennas are shown in Figs. 6(a)-(c). The radiation patterns are measured in the anechoic chamber with a measurement step illustrated in Fig. 6(d). Some positioning holes are drilled on the fixture to offer exact displacements (e.g., ± 20 mm, ± 40 mm, and ± 60 mm) for the feed source to achieve the scanning and symmetric radiation beams. The reflection coefficients of the three beam-steerable TA antennas are all measured when the radiation beam directs to different directions. It is found that all reflection coefficients are below -10 dB from 22 GHz to 33 GHz, which are not shown here for brevity.

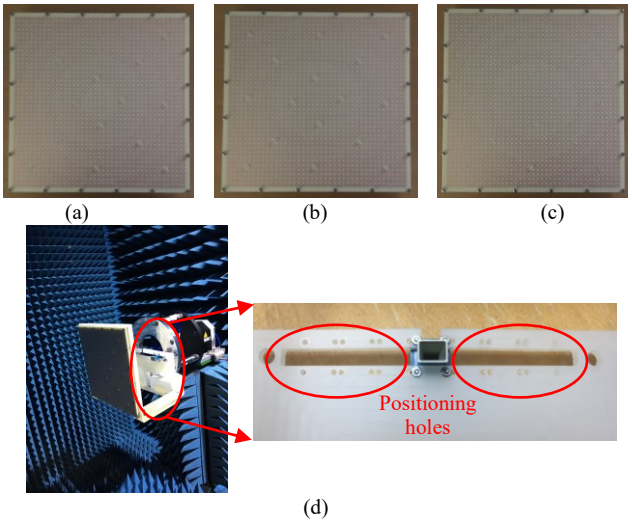

Fig. 6. Photographs and the measurement setup. The prototype of (a). The unifocal beam-steerable TA antenna. (b). The bifocal beam-steerable TA antenna. (c). The beam-steerable TA antenna enabled by the offset unifocal phase symmetry. (d). The measurement setup.

The scanning beams of the three beam-steerable TA antennas are measured at 25.0 GHz. As seen in Fig. 7, the radiation beams of all beam-steerable TA antennas can be steered from 0° to ± 30°. The measured realized gain of the unifocal beam-steerable TA antenna is 31.0 dBi at the broadside direction which is slightly smaller than the simulated result (31.5 dBi), the gain roll-off is around 5.1 dB which is very close to the simulation (5.3 dB), and the measured sidelobe levels of the scanning beams are -24.0 dB, -12.0 dB, -8.5 dB, and -10 dB as observed in Fig. 7(a). The measured gain roll-off of the bifocal beam-steerable TA antenna is around 1.3 dB, the maximum realized gain is around 25.0 dBi, and the measured sidelobe levels of the scanning beams at broadside and ± 10° are slightly higher than the simulated results as seen in Fig. 7(c). The measured realized gain of the beam-steerable TA antenna enabled by the offset unifocal phase symmetry is around 29.4 dBi at the broadside direction, the gain roll-off is 1.6 dB, and the measured sidelobe levels of the scanning beams are highly consistent with the simulated results as can be checked from Fig. 7(e). Moreover, the cross-pol. levels of the three beam-steerable TA antennas in the cut plane where the main beam steers are also measured and presented when the main beam is steered from 0° to 30°. As seen in Figs. 7(b), 7(d), and 7(f), the measured cross-pol. levels are all better than -22.5 dB for all scanning beams. The measured results presented in Fig. 7 sufficiently demonstrate that the beam-steerable TA antenna enabled by the offset unifocal phase symmetry can indeed achieve high realized gain, small gain roll-off, and suppressed sidelobe level.

The realized gains of the three beam-steerable TA antennas versus frequencies are also measured and compared with the simulated results when the main beam is at the broadside direction and steered to 30°. The measured results are slightly smaller than the simulated ones as seen in Fig. 8. When the main beam is at the broadside direction, the unifocal beam-steerable TA antenna can offer maximum realized gains, while the beam-steerable TA antenna enabled by the offset unifocal phase symmetry outperforms the unifocal and bifocal TA antennas when the main beam is steered to 30°.

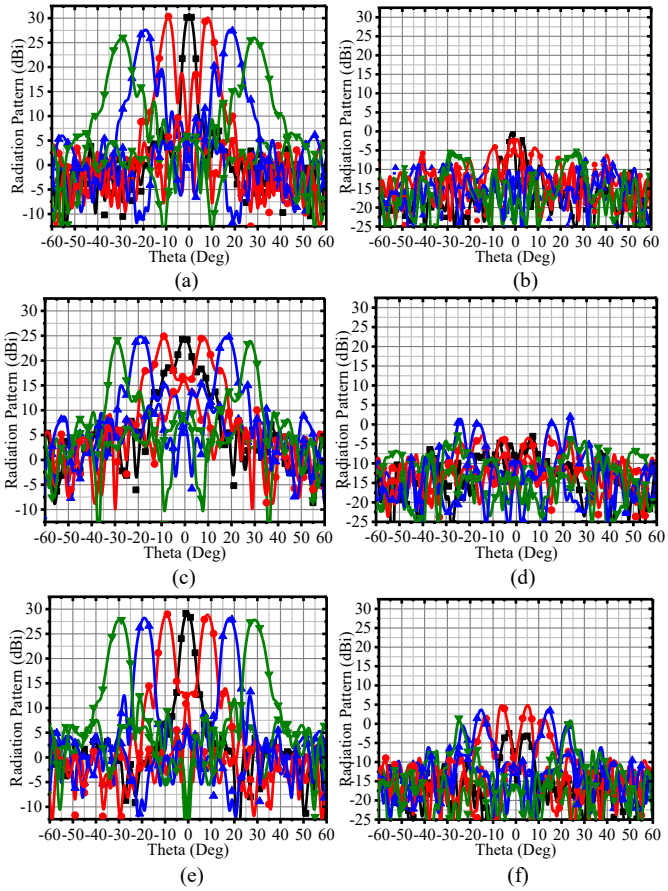

Fig. 7. The measured radiation patterns of the three beam-steerable TA antennas at 25.0 GHz. (a). Co-pol. of the unifocal beam-steerable TA antenna. (b). Cross-pol. of the unifocal beam-steerable TA antenna. (c). Co-pol. of the bifocal beam-steerable TA antenna. (d). Cross-pol. of the bifocal beam-steerable TA antenna. (e). Co-pol. of the offset unifocal phase symmetry enabled beam-steerable TA antenna. (f). Cross-pol. of the offset unifocal phase symmetry enabled beam-steerable TA antenna.

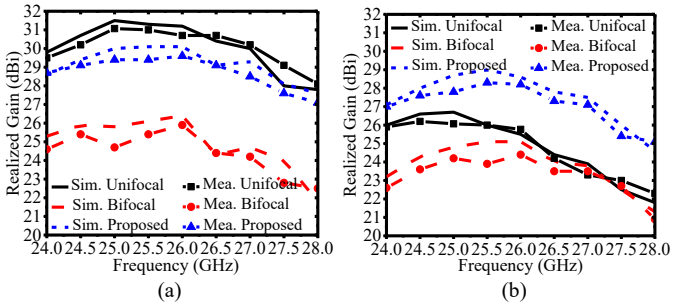

Fig. 8. The measured and simulated realized gains of the three beam-steerable TA antennas with frequencies. (a). The radiation beam at the broadside direction. (b). The radiation beam tilted 30°.

When the feed source is located at the center of the phase-shifting

phase, the main beam is always at the broadside direction across the frequency band, while the directions of the main beams will be slightly different with frequencies when the feed source is offset. Here, the beam squints of the three beam-steerable TA antennas are checked when the feed source is offset by +/- 60mm, where the beam squints of the unifocal, bifocal, and proposed beam-steerable TA antennas are 1°. 2°, and 2° from 24 GHz to 28 GHz, respectively.

IV. Discussion

A. Generality of the offset unifocal phase symmetry.

The concept of offset unifocal phase symmetry has turned out to be an effective solution to improve the performance of mechanically beam-steerable TA antennas from the simulations and measurements. According to the derivations of the offset unifocal phase symmetry presented in Section II-A, it should be also applicable to mechanically beam-steerable RA antennas to improve the performance, where the numerically verified improvements also follow the results observed from the mechanically beam-steerable TA antennas.

B. Extension of the concept of phase symmetry.

The phase shifts shown in Fig. 3(d) are not symmetric along $x = \pm y$, which will lead to asymmetric radiation performance when the feed source moves along the x- and y-direction. Here, the phase symmetry can be further adopted to make the phase shifts shown in Fig. 3(d) also symmetric with respect to $x = \pm y$ by imposing $\varphi(i,j) = \varphi(j,i)$ when $-100 \le i \le -1$, $1 \le j \le 100$, and $|i|>j$, therefore enabling the similar radiation beams when the feed source moves along the x- and y-direction. Moreover, the concept of phase symmetry can be further extended and leveraged to make some asymmetric components (e.g., electric field, phase, etc.) symmetric to obtain symmetric performance.

V. Conclusion

This paper introduces a concept of offset unifocal phase symmetry to improve the performance of mechanically beam-steerable TA antennas, which is also applicable to mechanically beam-steerable RA antennas. Three beam-steerable TA antennas have been simulated and measured to validate the effectiveness of the offset unifocal phase symmetry. The measured results agree well with the simulated results, where the beam-steerable TA antenna enabled by the offset unifocal phase symmetry can achieve a smaller gain roll-off than that of the unifocal beam-steerable TA antenna, higher realized gains than the counterparts of the bifocal beam-steerable TA antenna, and outperforms both unifocal and bifocal beam-steerable TA antennas in terms of the sidelobe levels of all scanning beams.

References

[1] W. Hong, *et al*., "Multibeam antenna technologies for 5G wireless communications," *IEEE Trans. Antennas Propag*., vol. 65, no. 12, pp. 6231-6249, Dec. 2017.

[2] B. Yang, Z. Yu, J. Lan, R. Zhao, J. Zhou, and W. Hong, "Digital beamforming-based massive MIMO transceiver for 5G millimeter-wave communications," *IEEE Trans. Micro Theory Tech*., vol. 66, no. 7, pp. 3403-3418, Jul. 2018.

[3] H. Kamoda, T. Iwasaki, J. Tsumochi, T. Kuki, and O. Hashimoto, "60-GHz electronically reconfigurable large reflectarray using single-bit phase shifter," *IEEE Trans. Antennas Propag*., vol. 59, no. 7, pp. 2524 - 2531, Jul. 2011.

[4] H. Yang, *et al*., "A 1-bit 10 x 10 reconfigurable reflectarray antenna: design, optimization, and experiment," *IEEE Trans. Antennas Propag*., vol. 64, no. 6, pp. 2246 - 2254, Jun. 2016.

[5] E. Carrasco, M. Barba, and J. A. Encinar, "X-band reflectarray antenna with switching-beam using PIN diodes and gathered elements," *IEEE Trans. Antennas Propag*., vol. 60, no. 12, pp. 5700 - 5708, Dec. 2012.

[6] A. Clemente, L. Dussopt, R. Sauleau, P. Potier, and P. Pouliguen, "Wideband 400-element electrically reconfigurable transmitarray in X band," *IEEE Trans. Antennas Propag*., vol. 61, no. 10, pp. 5017 - 5027, Oct. 2013.

[7] Y. Wang, S. Xu, F. Yang, and M. Li, "A novel 1 bit wide-angle beam scanning reconfigurable transmitarray antenna using an equivalent magnetic dipole element," *IEEE Trans. Antennas Propag*., vol. 68, no. 7, pp. 5691 - 5695, Jul. 2020.

[8] M. Wang, S. Xu, F. Yang, and M. Li, "Design and measurement of a 1-bit reconfigurable transmitarray with subwavelength H-shaped coupling slot elements," *IEEE Trans. Antennas Propag*., vol. 67, no. 5, pp. 3500 - 3504, May. 2019.

[9] G. Wu, S. Qu, and S. Yang, "Wide-angle beam-scanning reflectarray with mechanical steering," *IEEE Trans. Antennas Propag*., vol. 66, no. 1, pp. 172-181, Jan. 2018.

[10] P. Nayeri, F. Yang, and A. Z. Elsherbeni, "Bifocal design and aperture phase optimizations of reflectarray antennas for wide-angle beam scanning performance," *IEEE Trans. Antennas Propag*., vol. 61, no. 9, pp. 4588 - 4597, Sep. 2013.

[11] G. Wu, S. Qu, S. Yang, and C. Chan, "Low-cost 1-D beam-steering reflectarray with ± 70° scan coverage," *IEEE Trans. Antennas Propag*., vol. 68, no. 6, pp. 5009 - 5014, Jun. 2020.

[12] M. Taher Al-Nuaimi, A. Mahmoud, W. Hong, and Y. He, "Design of single-layer circularly polarized reflectarray with efficient beam scanning," *IEEE Antennas Wireless Propag Letts*., vol. 19, no. 6, pp. 1002-1006, Jun. 2020.

[13] P. Mei, S. Zhang, and G. F. Pedersen, "A low-profile and beam-steerable transmitarray antenna: design, fabrication, and measurement [Antenna Application Concer], *IEEE Antennas Propag Mag*., vol. 63, no. 5, pp. 88-103, Oct. 2021.

[14] M. Jiang, Z. Chen, Y. Zhang, W. Hong, and X. Xuan, "Metamaterial-based thin planar lens antenna for spatial beamforming and multibeam massive MIMO," *IEEE Trans. Antennas Propag*., vol. 65, no. 2, pp. 464 - 472, Feb. 2017.

[15] Y. Hu, W. Hong, and Z. Jiang, "A multibeam folded reflectarray antenna with wide coverage and integrated primary sources for millimeter-wave massive applications," *IEEE Trans. Antennas Propag*., vol. 66, no. 12, pp. 6875 - 6882, Dec. 2018.

[16] R. Xu, and Z. Chen, "A compact beamsteering metasurface lens array antenna with low-cost phased array," *IEEE Trans. Antennas Propag*., vol. 69, no. 4, pp. 1992 - 2002, Apr. 2021.

[17] G. Li, Y. Ge, and Z. Chen, "A compact multibeam folded transmitarray antenna at Ku-band," *IEEE Antennas Wireless Propag Letts*., vol. 20, no. 5, pp. 808-812, May. 2021.

[18] J. Yang, Y. Shen, L. Wang, H. Meng, W. Dou, and S. Hu, "2-D scannable 40-GHz folded reflectarray fed by SIW slot antenna in a single-layered PCB," *IEEE Trans. Microw. Theory Techn*., vol. 66, no. 6, pp. 3129 – 3135, Jun. 2018.

[19] M. Abbasi, M. Dahri, M. Jamaluddin, and N. Seman, "Millimeter wave beam steering reflectarray antenna based on mechanical rotation of array," *IEEE Access*, vol. 7, pp. 145685 – 145681, 2019.

[20] P. Mei, S. Zhang, and G. F. Pedersen, "A low-cost, high-efficiency and full-metal reflectarray antenna with mechanically 2-D beam-steerable capabilities for 5G applications," *IEEE Trans. Antennas Propag*., vol. 68, no. 10, pp. 6997 - 7006, Oct. 2020.

[21] X. Yang, *et al*., "A broadband high-efficiency reconfigurable reflectarray antenna using mechanically rotational elements," *IEEE Trans. Antennas Propag*., vol. 65, no. 8, pp. 3959 - 3966, Aug. 2017.

[22] D. McGrath, "Planar three-dimensional constrained lenses," *IEEE Trans. Antennas Propag*., vol. AP-34, no. 1, pp. 46-50, Jan. 1986.

[23] B. Rao, "Bifocal dual reflector antenna," *IEEE Trans. Antennas Propag*., vol. AP-22, no. 5, pp. 711-714, Sep. 1974.

[24] Z. Yu, Y. Zhang, S. He, H. Gao, H. Chen, and G. Zhu, "A wide-angle coverage and low scan loss beam steering circularly polarized folded reflectarray antenna for millimeter-wave applications," *IEEE Trans. Antennas Propag*., *Early Access*., DOI: 10.1109/TAP.2021.3118790.

[25] P. Mei, S. Zhang, and G. F. Pedersen, "A dual-polarized and high-gain X/Ka-band shared-aperture antenna with high aperture reuse efficiency," *IEEE Trans. Antennas Propag*., vol. 69, no. 3, pp. 1334-1344, Mar. 2021.

[26] [Online].https://www.pasternack.com/images/ProductPDF/PE9851B-2F-10.pdf

[27] A. Yu, F. Yang, A. Z. Elsherbeni, J. Huang, and Y. Rahmat-Samii, "Aperture efficiency analysis of reflectarray antennas," *Micro. Opt. Tech Lett.,* vol. 52, no. 2, pp. 364-372, Feb 2010.